Growth Behavior of Al-Doped TiO_2 Thin Films by Atomic Layer Deposition

Seong Keun Kim, Gyu Jin Choi, Jeong Hwan Kim, and Cheol Seong Hwang*

Department of Materials Science and Engineering and Inter-university Semiconductor Research Center, Seoul National University, Seoul 151-744, Korea

Received January 28, 2008

This study examined the effect of Al incorporation on the growth behavior of TiO_2 thin films deposited by atomic layer deposition (ALD) using $Al(CH_3)_3$, and $Ti(O\text{-}i\text{-}C_3H_7)_4$ as the precursors and O_3 as the reactant. Al-doped TiO_2 thin films were deposited at a growth temperature of 250 °C, which was within the ALD window for both precursors. Despite the discrete feeding of the Al precursor, Al ions easily diffused along the direction normal to the film surface forming a uniform Al-doped thin film, even during film growth. The Al concentration in the films increased with increasing Al precursor feeding ratio. However, the adsorption of the Ti precursor on the growing surface became less active after the incorporation of Al. Therefore, the growth rate of the Al-doped TiO_2 films decreased with increasing Al precursor feeding ratio because of the retarded chemisorption of the Ti precursor onto the Al−O and Al containing Ti−O surface. In contrast to the retarded adsorption of the Ti precursor on the Al−O surface, the adsorption of the Al precursor on the Ti−O surface was enhanced by ∼60% compared with that on the Al−O surface.

1. Introduction

Atomic layer deposition (ALD) has attracted considerable attention as a method for growing thin films for various applications on account of its excellent thickness controllability, conformal growth on the complex-shaped structures, uniform film growth on large area substrates, low growth temperature and very low pinhole density.[1–7] Although ALD usually has a drawback of a lower growth rate compared to other film growth methods, such as chemical vapor deposition, it can be compensated to some extent by the excellent large-area deposition and batch-type process capability. Therefore, ALD is used widely in the semiconductor industry for fabricating the capacitors in dynamic random access memory (DRAM) or gate dielectrics of the field effect transistor that require very accurate control of the film thicknesses.[8–10] In particular, ALD is very useful for growing capacitor dielectrics in DRAMs. This is because the DRAM capacitor uses three-dimensional structures, such as cylinder or stack structures with a severe aspect ratio, in order to increase the effective surface area.[11]

TiO_2 in the rutile phase exhibits a dielectric constant value $\sim$ 100,[12] and, thus, can be used in DRAMs with a design rule of <40 nm. However, the small band gap of ∼3.1 eV makes it difficult to control the leakage currents.[13] The authors recently reported that the appropriate incorporation of Al ions into TiO_2 films using an ALD method makes it possible to achieve a dielectric film with a minimum equivalent oxide thickness (t_{ox}, = t_{phy} × 3.9/dielectric constant, where t_{phy} is the physical thickness of the film) of 0.48 nm, while still guaranteeing a sufficiently low leakage current.[14] The t_{ox} of 0.48 nm was the smallest ever reported among the values for binary oxides. However, the impacts of Al incorporation on the growth behavior of TiO_2 thin films and the dependence of the cation composition on the different precursor pulse ratios have not been reported in detail. This is important because the dielectric constant of the films is dependent on the film composition.[14]

In ALD, the chemical reaction between the precursors and adsorbing surface is a key factor in controlling the growth behavior of the films. A transient behavior generally occurs during the initial growth in ALD.[15–19] This can be understood

* To whom correspondence should be addressed. E-mail: cheolsh@snu.ac.kr.

(1) Suntola, T. *Thin Solid Films* **1992**, *216*, 84.
(2) Leskelä, M.; Niinistö, L. In *Atomic Layer Epitaxy*; Suntola, T.; Simpson, M., Eds.; Blackie, Glasgow, 1994; p 1.
(3) Gordon, R. G.; Hausmann, D.; Kim, E.; Shepard, J. *Chem. Vap. Deposition* **2003**, *9*, 73.
(4) Suntola, T. In *Handbook of Crystal Growth*; Hurle, D. T. J., Ed; Elsevier Science: New York, 1994; Vol. 3, Chapter 14.
(5) Suntola, T. *Mater. Sci. Rep.* **1989**, *4*, 261.
(6) Leskelä, M.; Ritala, M. *Thin Solid Films* **2002**, *409*, 138.
(7) Puurunen, R. L. *J. Appl. Phys.* **2005**, *97*, 121301.
(8) Leskelä, M.; Ritala, M. *Angew. Chem., Int. Ed.* **2003**, *42*, 5548.
(9) Ritala, M. In *High-k Gate Dielectrics*; Houssa, M., Ed.; IOP: London, 2004; p 17.
(10) Kim, S. K.; Lee, S. Y.; Lee, S. W.; Hwang, G. W.; Hwang, C. S.; Lee, J. W.; Jeong, J. *J. Electrochem. Soc.* **2007**, *154*, D95.
(11) Kim, S. K.; Kim, K.-M.; Kwon, O. S.; Lee, S. W.; Jeon, C. B.; Park, W. Y.; Hwang, C. S.; Jeong, J. *Electrochem. Solid-State Lett.* **2005**, *8*, F59.
(12) Kim, S. K.; Kim, K.-M.; Kim, W. D.; Hwang, C. S.; Jeong, J. *Appl. Phys. Lett.* **2004**, *85*, 4112.
(13) Kim, S. K.; Lee, S. Y.; Seo, M.; Choi, G.-J.; Hwang, C. S. *J. Appl. Phys.* **2007**, *102*, 024109.
(14) Kim, S. K.; Choi, G.-J.; Lee, S. Y.; Seo, M.; Lee, S. W.; Han, J. H.; Ahn, H.-S.; Han, S.; Hwang, C. S. *Adv. Mater.* **2008**, *20*, 1429.
(15) Puurunen, R. L. *J. Appl. Phys.* **2005**, *97*, 121301.
(16) Ylilammi, M. *Thin Solid Films* **1996**, *279*, 124.
(17) Park, H.-S.; Min, J.-S.; Lim, J.-W.; Kang, S.-W. *Appl. Surf. Sci.* **2000**, *158*, 81.

10.1021/cm800280t CCC: $40.75
Published on Web 05/20/2008

from the coexistence of the original substrate and depositing materials as an adsorbing surface during initial growth. In cases where more than one component is incorporated during film growth, such as the Al-doped TiO_2 in this case or multication oxide thin films, different cations coexist on the adsorbing surface. In such cases, the growth behavior can become much more complicated. In addition, doped materials are supposed to diffuse along with the growing surface during deposition. This forces the chemical composition of the surface to change continuously. Therefore, an understanding on the growth behavior can be further complicated.

Film growth behaviors by ALD of binary oxides or nitrides have been frequently reported, but there are relatively fewer reports on the growth and characterization of multicomponent[20–24] or doped material film growth.[25–27] Multicomponent or doped materials are generally grown by the alternative feeding of the precursor of each component in ALD. In these cases, the film composition is controlled by the precursors feeding ratio. Hwang et al.[22] recently reported the ALD of $PbTiO_3$ films using lead bis(3-*N*,*N*-dimethyl-2-methyl-2-propanoxide) and Ti(O-*t*-$C_4H_9)_4$ as Pb and Ti precursors, respectively, and H_2O as the oxidant. They showed that the cation composition in the films was controlled by the precursor feeding ratio, and the growth rate of the films was enhanced in the ternary process compared with the growth of its component oxide films. Watanabe et al.[23] also reported similar results for $PbTiO_3$ thin films even though they used the other precursors ($Pb(C_{11}H_{19}O_2)_2$ and Ti(O-*i*-$C_3H_7)_2(C_{11}H_{19}O_2)_2$). Kwon et al.[24] reported the enhancement in the growth rate of the $SrTiO_3$ thin films by ALD compared with its component oxides ($Sr(C_{11}H_{19}O_2)_2$, Ti(O-*i*-$C_3H_7)_4$, and H_2O). For the growth of doped binary oxide thin films by ALD, Zr-doped TiO_2 films[25] for photocatalyst applications and Al- or B-doped ZnO films[26,27] for transparent conducting oxide applications have been reported. These studies focused mainly on optimizing the material properties by determining the appropriate doping concentrations. However, to the best of our knowledge, there has not been a systematic study on the growth behavior of these films by the incorporation of the dopant.

Therefore, this study examined the effects of Al-doping on the growth behavior of TiO_2 films by ALD. In particular, the chemisorption characteristics between the adsorbing surface and precursors were carefully investigated. The Al doping level in this study was quite high so that it might be considered that the films are solid solutions.

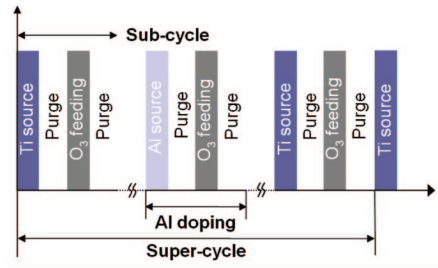

Figure 1. Schematic diagram of ALD process of Al-doped TiO_2 film.

2. Experimental Procedure

Undoped and Al-doped TiO_2 films were deposited using a traveling-wave type ALD reactor (Quros Co., Plus-100) on Ru(30 nm)/Ta_2O_5(8 nm)/SiO_2(100 nm)/Si substrates. The Ta_2O_5 film works as an adhesion-improving layer between the Ru and SiO_2 layers. Titanium tetrakis isoproxide (Ti(O-*i*-$C_3H_7)_4$, TTIP) and trimethyl aluminum ($Al(CH_3)_3$, TMA) were used as the Ti and Al precursors, respectively. O_3 with a concentration of 390 g/m^3 was used as the oxygen source. A mixture of O_2/N_2 with a flow rate of 700 sccm/5 sccm was introduced into an O_3 generator to produce O_3. The ALD windows of the component materials should overlap in case of growth of ternary or doped materials. It is known that ALD window of TiO_2 films from TTIP is below ~300 °C[28,29] and that for Al_2O_3 films from TMA is below ~400 °C.[30,31] Therefore, in this study the films was deposited at a growth temperature of 250 °C, which was within the ALD window for both precursors. It is impossible to continuously input the dopant atoms into the films during film growth due to the pulsed nature of ALD. Therefore, to incorporate Al ions into the films, an Al−O layer was incorporated discretely into the film by substituting one TTIP-O_3 cycle with one TMA-O_3 cycle in a single supercycle, as defined below. Figure 1 shows the pulse sequence used to deposit the Al-doped TiO_2 films. A supercycle consisted of a number of subcycles of TiO_2 (n_{Ti}) and a cycle of Al_2O_3. The Al_2O_3 cycle was employed at two-thirds of a supercycle. The Al concentration in the films was controlled by the Al and Ti precursor cycle ratio (R_{pc}, $[n_{Al}']/[n_{Al}' + n_{Ti}']$). n_{Ti}' and n_{Al}' are the numbers of total subcycles of Ti and Al precursors, respectively. R_{pc} was varied from 1/120 to 1/60. The Ti and Al precursor pulse times were 2 and 0.5 s, respectively. The purge time of each precursor was 3 and 20 s, respectively. The O_3 pulse time and purge time were 3 and 3 s, respectively. The other details of the ALD process are reported elsewhere.[12–14]

The physical thickness of the films was measured by ellipsometry, which was confirmed by high-resolution transmission electron microscopy. The layer density of Ti ions in the films was measured by X-ray fluorescence spectroscopy (XRF). The [Al]/[Al+Ti] atomic ratio of the films was investigated by an inductively coupled plasma spectroscopy-atomic emission spectrometer (ICP-AES).

3. Results and Discussions

Figure 2a shows the variations in film thickness as a function of the number of total subcycles ($n_{Ti}' + n_{Al}'$). Figure 2a also shows the thickness of the undoped TiO_2 films for comparison. The growth rates of the Al-doped TiO_2 films were calculated from the slope of the linear fit graphs shown

(18) Puurunen, R. L. *Chem. Vap. Deposition* **2003**, *9*, 249.
(19) Haukka, S.; Lakomaa, E.; Suntola, T. *Stud. Surf. Sci. Catal.* **1999**, *120*, 715.
(20) Kim, J.-H.; Kim, J.-Y.; Kang, S.-W. *J. Appl. Phys.* **2005**, *97*, 093505.
(21) Harjuoja, J.; Kosola, A.; Putkonen, M.; Niinistö, L. *Thin Solid Films* **2006**, *496*, 346.
(22) Hwang, G. W.; Lee, H. J.; Lee, K.; Hwang, C. S. *J. Electrochem. Soc.* **2007**, *154*, G69.
(23) Watanabe, T.; Hoffmann-Eifert, S.; Mi, S.; Jia, C.; Waser, R.; Hwang, C. S. *J. Appl. Phys.* **2007**, *101*, 014114.
(24) Kwon, O. S.; Kim, S. K.; Cho, M.; Hwang, C. S.; Jeong, J. *J. Electrochem. Soc.* **2005**, *152*, C229.
(25) Qiu, S.; Starr, T. L. *J. Electrochem. Soc.* **2007**, *154*, H472.
(26) Yousfi, E. B.; Weinberger, B.; Donsanti, F.; Cowache, P.; Lincot, D. *Thin Solid Films* **2001**, *387*, 29.
(27) Yamamoto, Y.; Saito, K.; Takahashi, K.; Konagai, M. *Sol. Energy Mater. Sol. Cells* **2001**, *65*, 125.
(28) Kim, W. D.; Hwang, G. W.; Kwon, O. S.; Kim, S. K.; Cho, M.; Jeong, D. S.; Lee, S. W.; Seo, M. H.; Hwang, C. S.; Min, Y.-S.; Cho, Y. J. *J. Electrochem. Soc.* **2005**, *152*, C552.
(29) Ritala, M.; Leskelä, M.; Niinistö, L.; Haussalo, P. *Chem. Mater.* **1993**, *5*, 1174.
(30) Higashi, G. S.; Fleming, C. G. *Appl. Phys. Lett.* **1989**, *55*, 1963.
(31) Kim, S. K.; Hwang, C. S. *J. Appl. Phys.* **2004**, *96*, 2323.

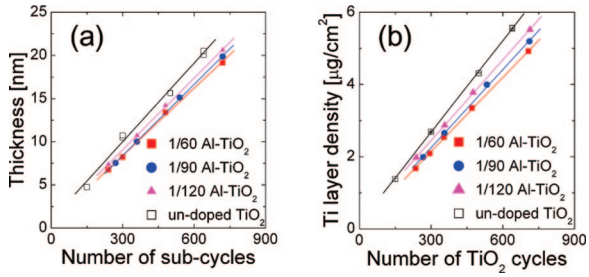

Figure 2. Variations in the (a) film thickness as a function of the number of subcycles and the (b) Ti layer density as a function of the number of TiO_2 cycles on Ru substrates with various R_{pc}.

in Figure 2a. The growth rate of the undoped TiO_2 film was 0.033 nm/cycle and those of the Al-doped TiO_2 films with an R_{pc} of 1/60, 1/90, and 1/120 were 0.026, 0.027, and 0.028 nm/cycle, respectively. The growth rate of the TiO_2 film decreased with increasing R_{pc}. The growth rate decreases by more than 15% because of the incorporation of Al even when the R_{pc} was as low as 1/120. It was reported that the growth rate of Al_2O_3 thin films grown by ALD with TMA and O_3 is approximately 0.09 nm/cycle at a growth temperature of 250 °C.[32–34] Considering the higher growth rate of Al_2O_3 thin films than TiO_2 films, it is expected that the growth rate of TiO_2 films would be increased by the incorporation of Al. However, the growth rate of the Al-doped TiO_2 films actually decreased with increasing R_{pc}. A further increase in the R_{pc} results in a degradation of the crystalline quality of the TiO_2 film and the formation of separate phases not uniform Al-doped TiO_2 films. Therefore, the R_{pc} was limited to 1/60 in this experiment.

It should be noted that the Al concentration was uniform along the direction normal to the surface in all cases, even though the Al had been fed discretely.[14] This was confirmed by the Auger electron spectroscopy, transmission electron microscopy, and X-ray photoelectron spectroscopy.[14] This suggests that Al easily diffuses along that direction during ALD even at such a low temperature, which has an important influence on the growth behavior of the TiO_2 layer as will be discussed later.

Figure 2b shows the variation in the Ti layer density obtained by XRF as a function of n_{Ti}' at various R_{pc} values. The increase in the Ti ion layer density of the undoped TiO_2 film per cycle was 8.44 ng/(cm^2 cycle), and Ti ion layer densities of the Al-doped TiO_2 films with an R_{pc} of 1/60, 1/90, and 1/120 were 6.84, 7.21, and 7.44 ng/(cm^2 cycle), respectively. The increase in the Ti layer density per cycle of the films decreased with increasing R_{pc}, which reflects the growth rate shown in Figure 2a.

As discussed previously, Al ions diffuse throughout the film thickness and form uniform Al-doped TiO_2 not a TiO_2 film containing a thin AlO_x layer in the middle. This is believed to be due to the excess oxygen composition of the TiO_2 film (Ti:O ratio ~1: 2.2),[13] where a high concentration of Ti-site vacancies works as an Al diffusion path. First principles calculations showed that the Al ions found energetically favorable sites on the TiO_2 surface compared with the positions inside the TiO_2 bulk. Therefore, it appears that there are the thermodynamic driving force (energetically favorable surface positions) and kinetic path (Ti-site vacancies) for the easy diffusion of Al during ALD. It was reported that the Al concentration on the film surface is indeed higher than that in the bulk even though there is a uniform Al distribution inside the film.[14] Therefore, it appears that the incorporated Al ions at two-thirds of one supercycle were driven to the surface during the subsequent ALD cycles of TiO_2. Some of the Al ions remained inside the film, which constitutes the bulk Al concentration. Therefore, the presence of Al ions on the film surface influences the chemisorption behaviors of the Ti-precursors, as shown in Figure 2.

The ionic radius of Al^{3+} (0.050 nm) is smaller than that of Ti^{4+} (0.068 nm).[35,36] Therefore, Al ions in the TiO_2 films might be located at the interstitial positions or they can substitute for Ti ions.

Because the Al cycle is incorporated discretely at a certain time (two-thirds) in a single supercycle, and the level of Ti incorporation on the Al-containing Ti−O surface was retarded compared with that on the pure Ti−O surface, as shown in Figure 2, it can be anticipated that the growth rate of TiO_2 may not be constant during a single supercycle. It should be lowest immediately after the Al−O cycle and increase as the rest of the Ti cycle repeats because the surface Al concentration must be highest immediately after the Al−O cycle. The Ti cycles immediately after the Al−O cycle were influenced more (chemisorption was largely retarded by the temporarily higher Al concentration) compared to the Ti cycles far after or before the Al−O cycle. These Ti cycles might be called as transition cycles. After the transition cycles, the TiO_2 growth rate recovers its saturation growth rate (GR_{sat}). However, it should be noted that this GR_{sat} is still smaller than the growth rate of pure TiO_2 due to the presence of Al on the growing surface. To understand this more quantitatively, the following assumption was made, and the growth behavior was further analyzed on the basis of this assumption. There is a certain saturation concentration of Al on the growing surfaces, which is preserved during the whole growth process with the exception of the transition period. This saturation concentration of Al is regardless of the R_{pc}. In other words, it is a type of intrinsic property of the growing surface. It was mentioned that Al ions migrate to energetically favorable locations on the surface than inside the bulk of TiO_2. This may have some correlation with the hypothesis. According to this hypothesis, the GR_{sat} should be independent of the R_{pc}. Considering this hypothesis, Figure 3a shows a schematic diagram of the actual Ti layer density variations as a function of n_{Ti}' for a R_{pc} of 1/90 shown in Figure 2b. Because the Ti layer density of the films was measured experimentally with the number of super cycles, the experimental data were included as closed circles and

(32) Kim, J. B.; Kwon, D. R.; Chakrabarti, K.; Lee, C.; Oh, K. Y.; Lee, J. H. *J. Appl. Phys.* **2002**, *92*, 6739.
(33) Kim, S. K.; Lee, S. W.; Hwang, C. S.; Min, Y.-S.; Won, J. Y.; Jeong, J. *J. Electrochem. Soc.* **2006**, *153*, F69.
(34) Elliott, S. D.; Scarel, G.; Wiemer, C.; Fanciulli, M.; Pavia, G. *Chem. Mater.* **2006**, *18*, 3764.
(35) Omari, M. A.; Sorbello, R. S.; Aita, C. R. *J. Appl. Phys.* **2006**, *99*, 123508.
(36) Zaitsu, S.-I.; Jisuno, T.; Nakatsuka, M.; Yamanaka, T.; Motokoshi, S. *Appl. Phys. Lett.* **2002**, *80*, 2442.

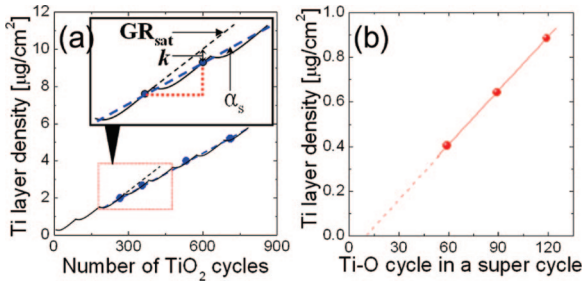

Figure 3. (a) Schematic diagram of the actual Ti layer density variations as a function of n_{Ti} for Al-doped TiO_2 film with an R_{pc} of 1/90. k is the retardation factor for Ti growth by the presence of Al on the growing surface, α_s is the average increment of Ti layer density per number of TiO_2 cycles, and the solid line indicates the variations of the actual Ti layer density of the films, (b) the variation in the Ti layer density as a function of the number of the subcycles of TiO_2 deposition in a supercycle.

its linear fitting line is also included as a blue dashed line. This blue dashed line corresponds to the data shown in Figure 2b. According to this model, the Ti layer density (ρ) as a function of n_{Ti}' for an R_{pc} of 1/60 and 1/90 after the transition cycles can be expressed as 1 and 2, respectively.

$$\rho = GR_{sat} n_{Ti}' - k[(n_{Ti}' + 20)/60] \quad (1)$$

$$\rho = GR_{sat} n_{Ti}' - k[(n_{Ti}' + 30)/90] \quad (2)$$

where k is retardation factor for Ti growth by the presence of Al on the growing surface, and [ ] is the Gaussian symbol. The Gaussian symbol mathematically expresses the total number of Al cycles in the growth of the films. Terms such as 20/60 and 30/90 were used to take into account the fact that the Al cycle was inserted at two-thirds of a super cycle. For example, $[(n_{Ti}' + 20)/60]$ is 2 for $n_{Ti}' = 120$. It needs to be reminded that eqs 1 and 2 were based on the hypothesis given above, and they are actually independent of the absolute value of k. The GR_{sat} and k values calculated from the given data points for the two R_{pc} values were 7.95 ng/(cm^2 cycle) and 66 ng/cm^2, respectively. The hypothesis given above can be verified from the much smaller k value compared with the total amount of Ti deposited in a single super cycle (~410 and ~650 ng/cm^2 for the R_{pc} of 1/60 and 1/90, respectively). Here, the k value could be understood as the extra-reduced amount of Ti deposition during the transition period by the temporarily higher Al concentration immediately after the Al-cycle compared with the case where growth proceeded with the same GR_{sat}. (See Figure 3a).

It should be also noted that the 7.95 ng/(cm^2 cycle) of GR_{sat} is still lower than that of the growth rate of pure TiO_2 films (8.44 ng/(cm^2 cycle)).

The above hypothesis could also be verified as follows. Figure 3b shows the variations in the Ti layer density as a function of n_{Ti}. Here, the y-axis values indicate the increase in the Ti layer density per supercycle of the Al-doped TiO_2 film with a R_{pc} of 1/60, 1/90, and 1/120. The increase in Ti layer density per supercycle was calculated by multiplying the slopes in Figure 2b by n_{Ti}. It can be understood that the three data points form an almost linear line suggesting that the GR_{sat} was independent of R_{pc}. This suggests that all the data points in Figure 3b belong to the saturated growth region. This can be understood more clearly from the following.

It is essential to have a slope (α_s) in Figure 2b for Al-doped TiO_2 films as a function of n_{total}, which is the sum of n_{Ti} and n_{Al} of a super cycle. However, eqs 1 and 2 contain the Gaussian symbol, so that the other method is necessary. Considering the inset figure of Figure 3a, α_s can be given as eq 3.

$$\alpha_s = (n_{Ti} GR_{sat} - k)/n_{Ti} \quad (3)$$

Therefore, the Ti layer density in Figure 3b should be given as eq 4.

$$\rho = n_{Ti}(n_{Ti} GR_{sat} - k)/n_{Ti} = n_{Ti} GR_{sat} - k \quad (4)$$

Therefore, the data points in Figure 3 (b) should form a straight line if the GR_{sat} is independent of R_{pc} in this region, as was indeed the case. The calculated saturation growth rate from the slope of the linear fitting of Figure 3 (b) was 8.03 ng/(cm^2 cycle), which is almost identical to the value achieved from eqs 1 and 2 (7.95 ng/(cm^2 cycle)). The y-axis intercept of Figure 3b corresponds to k and the calculated value from a linear extrapolation was ~71 ng/cm^2, which also corresponds well to the 66 ng/cm^2 given above.

The GR_{sat} of the 8.03 ng/(cm^2 cycle) of the Al-doped TiO_2 films is independent of n_{Ti} in this experimental range and is lower than that (8.44 ng/(cm^2 cycle)) of the undoped TiO_2 films. This suggests that the Al concentration on the growing film surface was constantly maintained after the transition period in a single supercycle, and the value was almost independent of R_{pc} in this experimental condition.

Fully oxidized Ti and Al ions are not isovalent, and have different radii (0.068 and 0.050 nm for Ti^{4+} and Al^{3+}, respectively).[35,36] Consequently, bulk TiO_2 and Al_2O_3 have no common lattice structure at any temperature or pressure[36] and do not form a solid solution. Moreover, only one high-temperature, enthalpy-stabilized compound,[37] Al_2TiO_5, is formed when they are intermixed. On the other hand, it was reported that there is a strong affinity for the formation of Ti−O−Al bonds across the a TiO_2−Al_2O_3 interface[38,39] with a structural adjustment to satisfy charge balance.[40,41] Therefore, it can be understood that Al and Ti ions in the film might be well-intermixed because the amount of Al_2O_3 introduced by a single cycle in this study was less than one monolayer.

It has to be mentioned that the very first cycles of the film growth (20 and 30 cycles for the 1/60 and 1/90 cases, respectively) proceed without the influence of Al incorporation because the first Al cycle is not yet executed. Therefore, the analysis given above does not apply to these steps. However, the portion of these initial cycles to the total number of cycles in this experiment (150−750) is quite small so that the error that might be caused from these cycles is negligible.

The growth behavior of the films was further examined by calculating the Al concentration in the films from the

(37) Navrotsky, A. *Am. Mineral.* **1975**, *60*, 249.
(38) Sanchez-Agudo, M.; Soriano, L.; Quiros, C.; Avila, J.; Sanz, J. M. *Surf. Sci.* **2001**, *482−485*, 470.
(39) Sanchez-Agudo, M.; Soriano, L.; Quiros, C.; Abbate, M.; Roca, L.; Avila, J.; Sanz, J. M. *Langmuir* **2001**, *17*, 7339.
(40) Steveson, M.; Bredow, T.; Gerson, A. R. *Phys. Chem. Chem. Phys.* **2002**, *4*, 358.
(41) Gesenhues, U.; Rentschler, T. *J. Solid State Chem.* **1999**, *143*, 210.

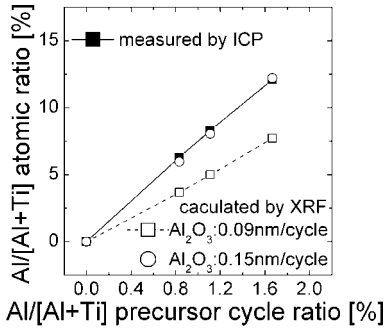

Figure 4. Al/[Al+Ti] atomic ratios in the films as a function of the R_{pc}. The values were measured by ICP-AES and calculated by amount of Ti ions measured by XRF and the amount of Al ions of Al_2O_3 film with the assumed growth rate of 0.09 and 0.15 nm/cycle.

expected growth rate, and theoretical density of the Al_2O_3 layer and the increase in the Ti layer density measured by XRF. The results were compared with the Al composition measured by ICP-AES. The expected growth rate of the Al−O layer was changed iteratively until the two results become identical because no X-ray signal for Al was detected in this XRF system. Two terms were assumed for this calculation. First, the amount of Al ions incorporated in a single Al−O cycle during Al-doped TiO_2 film growth is identical to that of pure Al_2O_3 film growth. Second, the density of the Al_2O_3 films grown by ALD is identical to the bulk density of α-Al_2O_3 (3.987 g/cm^3). On the basis of the bulk density of rutile TiO_2 (4.250 g/cm^3) and that of α-Al_2O_3, the layer density increase of each cation per cycle can be calculated using the thickness growth rate of TiO_2 and Al_2O_3 films grown at 250 °C (0.033 and 0.09 nm/cycle, respectively). The values for TiO_2 and Al_2O_3 were 8.41 and 18.99 ng/(cm^2 cycle), respectively. It should be noted that the calculated value for TiO_2 is similar to the experimental value (8.44 ng/(cm^2 cycle)) for the undoped TiO_2 film shown in Figure 2b. This means that TiO_2 films with a density close to the theoretical value are formed by the present ALD process.

The molar increase in Ti ions per cycle in the Al-doped TiO_2 with an R_{pc} value of 1/60, 1/90, and 1/120 and the undoped TiO_2, which was converted from the data measured by XRF in Figure 2b, were 1.428, 1.505, 1.553, and 1.762 $\times$ 10^{-10} mol/(cm^2 cycle), respectively. The calculated value for Al ions in a single Al−O cycle was 7.039 $\times$ 10^{-10} mol/(cm^2 cycle). From these values, the calculated Al/[Al+Ti] atomic ratios of the Al-doped TiO_2 films with an R_{pc} of 1/120, 1/90, and 1/60 were 3.67, 4.99, and 7.71%, respectively. These values are shown in Figure 4 as open square symbols with the experimental results measured by ICP-AES (closed square symbol). The values calculated using the above method based on the XRF results were much lower than the values measured by ICP-AES. This means that the amount of Al ions incorporated per cycle in the growth of an Al-doped TiO_2 film is larger than that in the pure Al_2O_3 growth process where the growth rate is 0.09 nm/cycle. When the growth rate of the Al−O layer in the Al-doped TiO_2 film growth was assumed to be 0.15 nm/cycle, the calculated and measured atomic ratios coincide well, as shown in Figure 4. It should be noted that this growth rate is based on the assumption of the theoretical density of α-Al_2O_3, which is barely the case. Therefore, the absolute number is not significant. The important point is that the growth rate of the Al−O layer on the Ti−O surface is higher (by more than 60%) than that on the Al−O surface. This is in contrast to the retarded growth of the Ti−O layer on the Al−O (or Al-containing Ti−O) surface, as shown previously. The reasons for the retarded and enhanced growth of Ti−O on the Al−O or the Al-containing Ti−O layer and the Al−O layer on the Ti−O or the Al-containing Ti−O layer, respectively, are not completely understood. Although an unequivocal understanding on the factors that affect the growth rate in an ALD process is usually difficult, it is certain that the growth rate is influenced by the surface density of chemisorption sites and the molecular dimension of the precursors. Therefore, a further in-depth investigation of these aspects will be needed.

4. Conclusions

The growth behavior of Al-doped TiO_2 films grown by ALD was investigated. The Al concentration in the films could be controlled by varying the R_{pc}. The growth rate of the Al-doped TiO_2 films decreased with increasing R_{pc} because of the retarded chemisorption of the Ti precursor onto the Al−O and Al containing Ti−O surface. Although the Al−O cycle was inserted discretely during deposition, Al ions diffused easily into the films during film growth, and Al ions were distributed uniformly in the films, resulting in an Al-doped TiO_2 not an Al_2O_3/TiO_2 nanolaminated film. The retardation in the growth rate of the Ti−O layer on the Al−O layer was serious during the transition cycles immediately after the Al−O cycle, which were $\lesssim$15% of the total cycles in a single supercycle. After the transition cycles, the Ti−O growth rate saturated to a common value, which is $\sim$5% lower than that of pure TiO_2 growth, regardless of the R_{pc}. It appears that a certain constant Al concentration was maintained on the growing film surface during the saturated growth stage in each super cycle. The rest of the Al distributed in the film contributed to the Al doping in the film. The Al precursor adsorption was enhanced on the Ti−O surface compared with the Al−O surface, which is in contrast to the fact that the adsorption of the Ti precursor was inhibited on an Al−O surface compared with a Ti−O surface.

It is believed that the methodology used in this study to understand the influence of the intermittent doping stage on the growth of the matrix phase can be applied not only to this case but also many other cases where doping or complex film growth by the ALD process is essential.

Acknowledgment. The work was supported by the system IC 2010 program of the Korean government.

CM800280T